Electronic Supplementary -2

to the paper

CROZET RISE, INDIAN OCEAN (PETROLOGY, GEOCHEMISTRY AND GEODYNAMIC FEATURES OF FORMATION)

N.M. Sushchevskaya, V.D. Shcherbakov, E.P. Dubinin, T.A. Shishkina, B.V. Belyatsky, K.A. Lorenz, M.O. Anosova, D. Yu. Bolshiyanov

Figure S1

Fig. S1. Outcrop of a basanite lava flow on the northeastern coast of Possession Island (Crozet Rise), from which the studied sample P-1-6 was collected (coordinates of the sampling point: 46°23'29" S, 51°48'28" E) during the International Antarctic Circumpolar Expedition (ACE) in 2017 on the R/V Akademik Treshnikov. Photo by D.Yu. Bolshiyanov.

Figure S2

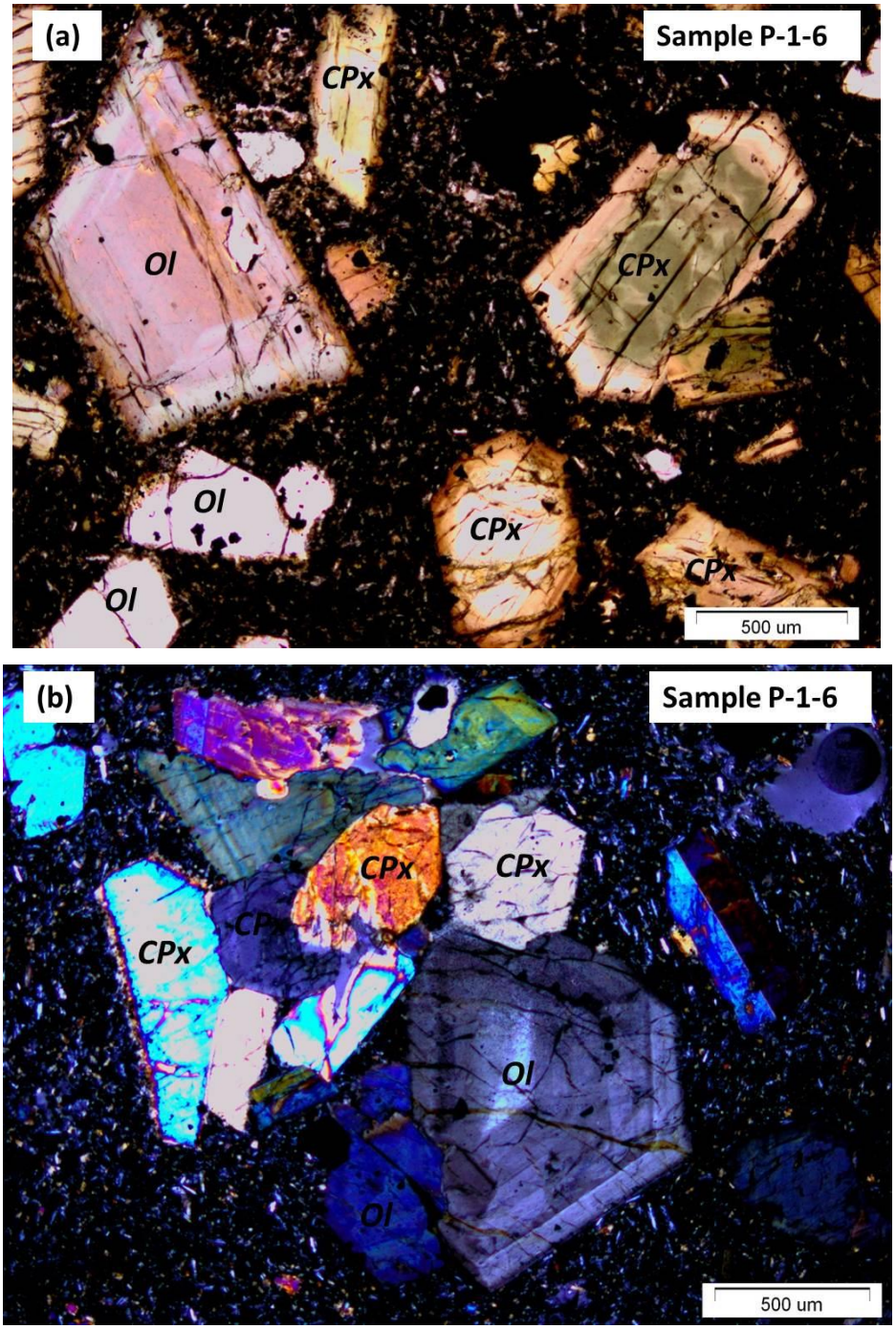

Fig. S2. Micrographs of a thin section of the Possession Island basanite (sample P-1-6) taken in transmitted light (a), and with crossed nicols (b). Phenocrysts of olivine and clinopyroxene with spinel inclusions are distributed in the groundmass, composed of microlites of clinopyroxene, plagioclase, olivine and titanomagnetite. *Ol* is olivine, *CPx* is clinopyroxene.

Figure S3

Phenocrysts and mineral inclusion associations in basanite P-1-6 from Possession Island. The mineral compositions were determined by TESCAN at GEOKHI RAS (full tables with mineral phase compositions are given in ***Electronic Supplementary-1***). *CPx* – clinopyroxene, *Ol* – olivine, *Ti-Mt* – titanomagnetite, *Spinel* – spinel.

Fig. S3-a. Association-1

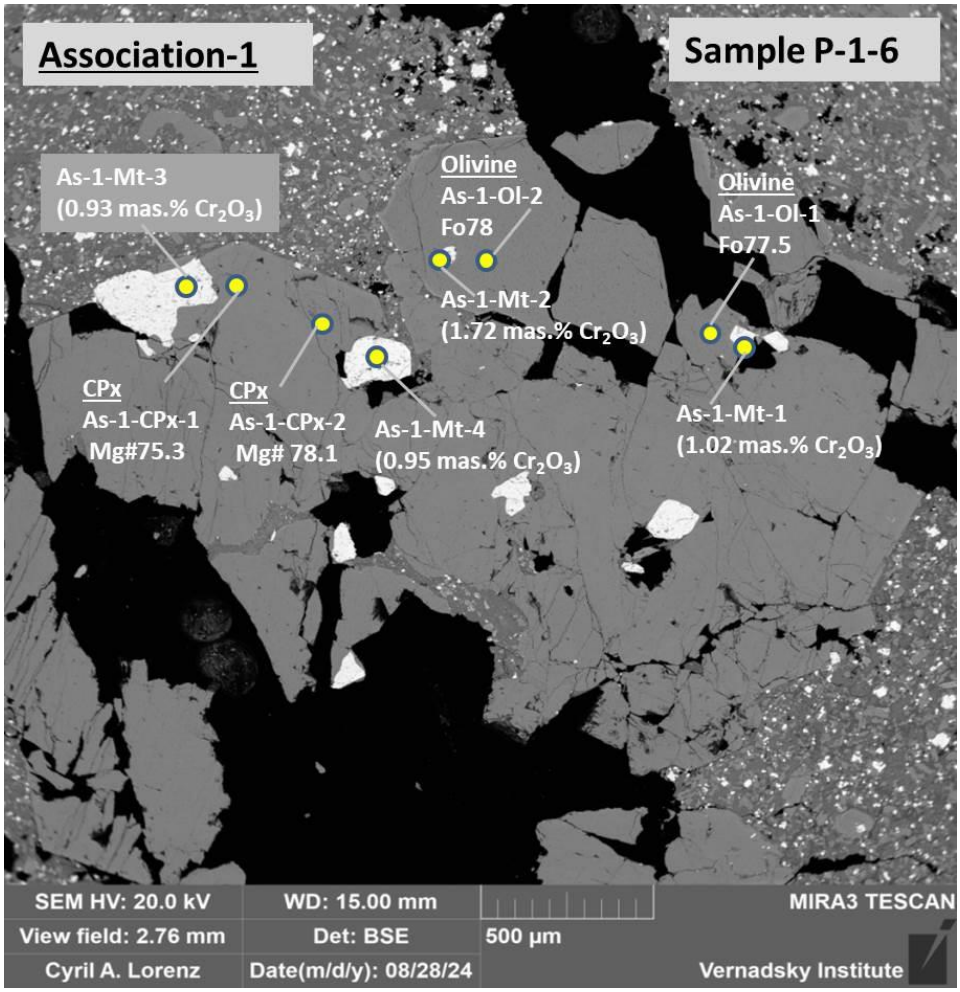

Phase	Analysis ID	SiO_2 (mas. %)	TiO_2 (mas. %)	Al_2O_3 (mas. %)	FeO-t (mas. %)	MnO (mas. %)	MgO (mas. %)	CaO (mas. %)	Na_2O (mas. %)	Cr_2O_3 (mas. %)	V_2O_3 (mas. %)	Total (mas. %)	Mg# (mol %)	Number of analyses
Ol	As-1-OL-1	38.62			20.84	0.40	40.28	0.26				100.4	77.5	2
Ol	As-1-OL-2	38.48			20.57	0.47	40.46	0.24				100.2	77.8	2
CPx	As-1-CPx-1	45.50	3.20	8.90	7.46	0.17	12.74	21.92	0.56			100.5	75.3	1
CPx	As-1-CPx-2	48.72	2.21	6.32	6.86		13.76	22.23	0.49			100.6	78.1	1
Ti-Mt	As-1-Mt-1	0.24	15.60	8.12	64.67	0.59	5.99			1.02	0.46	96.7		1
Ti-Mt	As-1-Mt-2	0.19	13.59	7.77	64.55	0.45	6.80			1.72	0.54	95.6		1
Ti-Mt	As-1-Mt-3	0.23	13.93	8.01	64.73	0.51	6.54			0.93	0.56	95.4		1
Ti-Mt	As-1-Mt-4	0.29	14.15	7.84	64.80	0.58	5.91			0.95	0.48	95.0		1

Fig. S3-b. Association-2

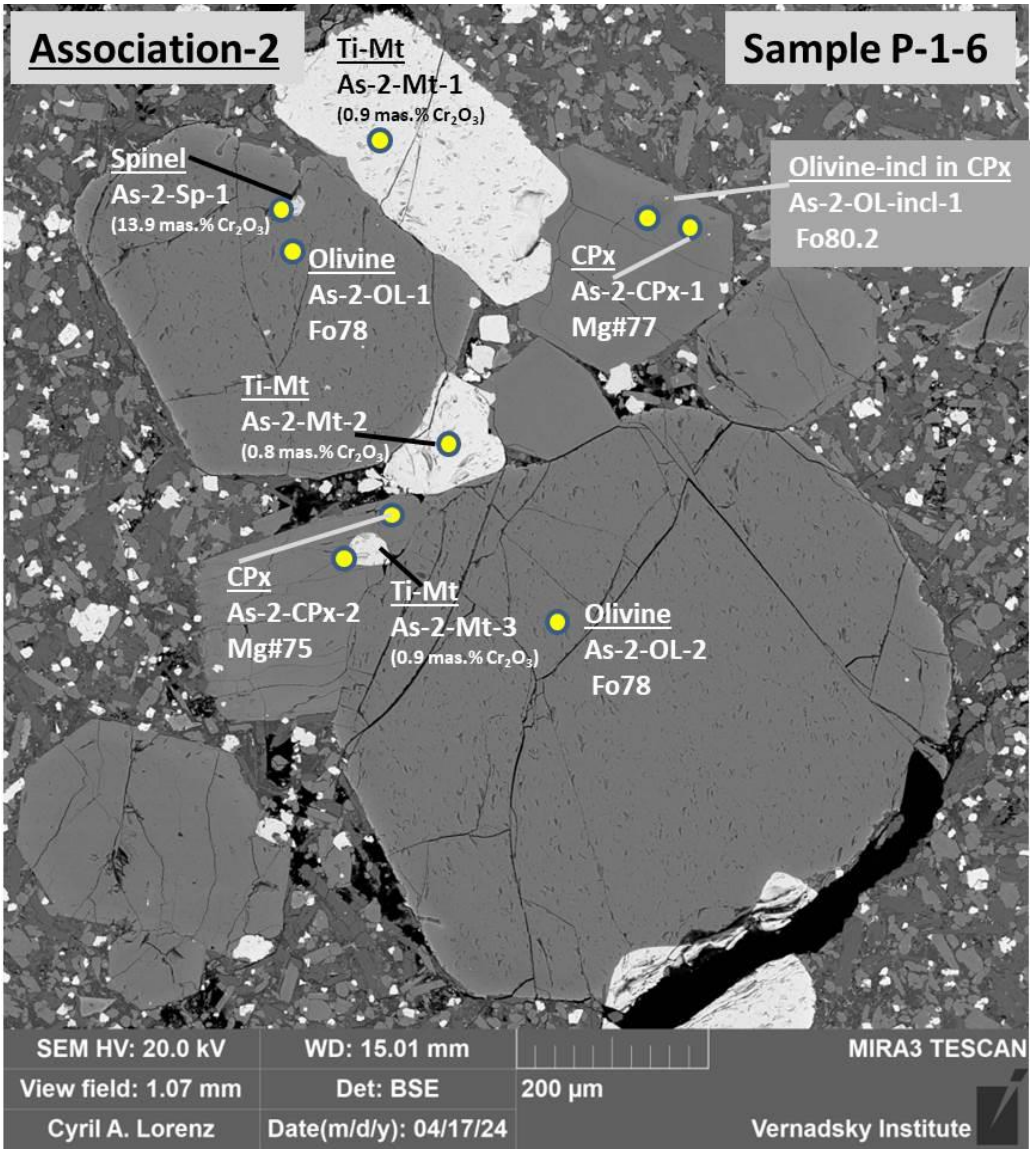

Phase	Analysis ID	SiO_2 (mas.%)	TiO_2 (mas.%)	Al_2O_3 (mas.%)	FeO-t (mas.%)	MnO (mas.%)	MgO (mas.%)	CaO (mas.%)	Na_2O (mas.%)	Cr_2O_3 (mas.%)	NiO (mas.%)	V_2O_3 (mas.%)	Total (mas.%)	Mg# (mol%)	Number of analyses
Ol	As-2-OL-1	38.64			20.47	0.46	40.26	0.25					100.1	77.8	1
Ol	As-2-OL-2	38.71			20.37	0.51	40.45	0.31					100.4	78.0	1
Ol	As-2-OL-incl-1	38.58	0.10	0.08	18.30	0.36	41.61	0.52			0.20		99.7	80.2	2
CPx	As-2-CPx-1a	47.40	2.36	7.00	7.21	0.17	13.30	21.90	0.57				99.8	76.7	2
CPx	As-2-CPx-2	45.08	2.94	8.00	7.41		12.50	21.72	0.51				98.4	75.0	1
(Cr)-Sp	As-2-Sp-1	0.24	4.62	14.06	54.56	0.52	7.39			13.92		0.41	95.7		1
Ti-Mt	As-2-Mt-1	0.19	14.63	7.79	66.28	0.58	5.88			0.85		0.50	96.7		1
Ti-Mt	As-2-Mt-2	0.17	15.23	7.87	64.26	0.63	5.60			0.79		0.60	95.2		1
Ti-Mt	As-2-Mt-3	0.16	13.17	7.58	64.06	0.44	6.81	0.21		0.86		0.52	93.9		1

Fig. S3-c. Association-3

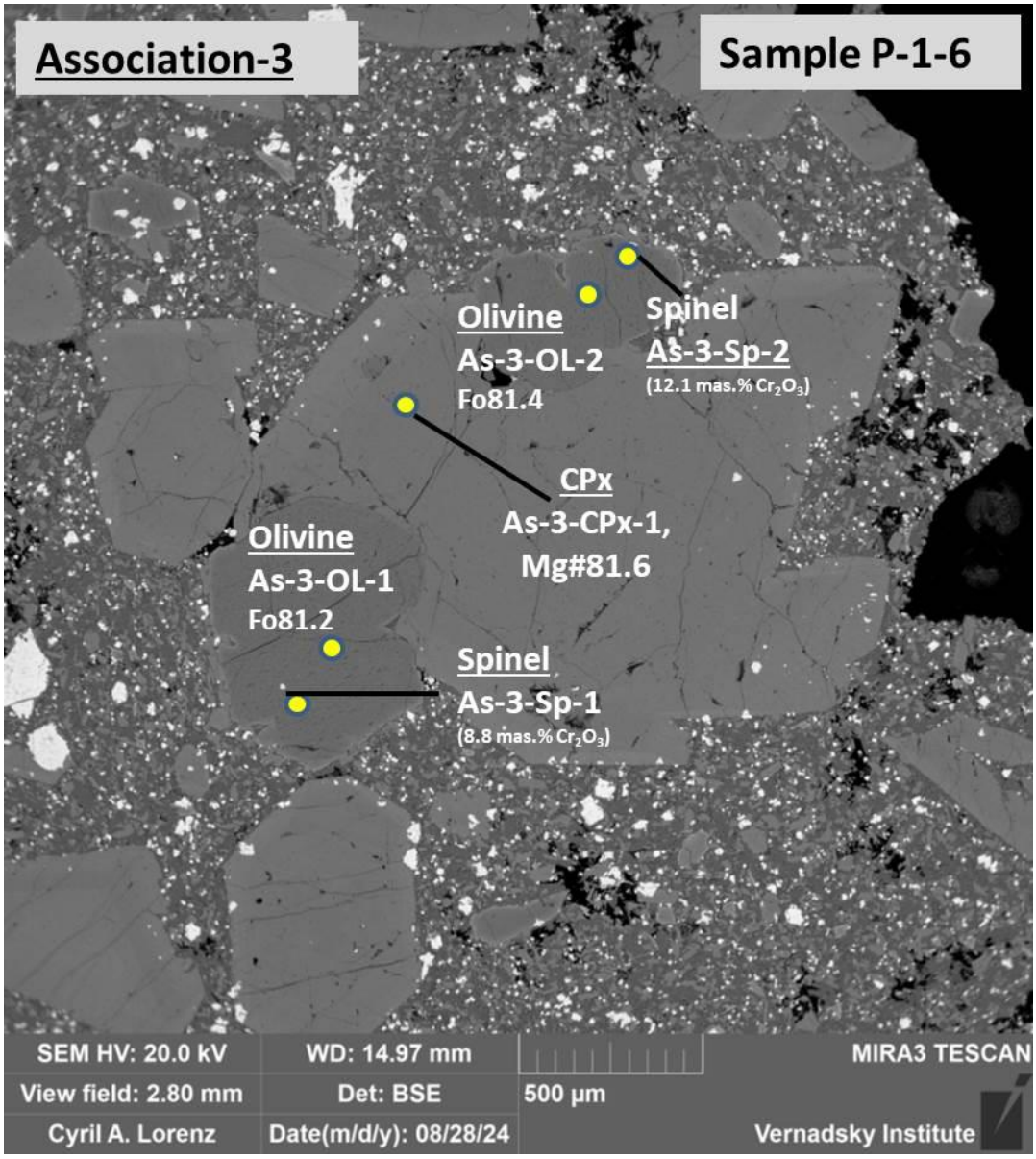

Phase	Analysis ID	SiO_2 (mas. %)	TiO_2 (mas.%)	Al_2O_3 (mas. %)	FeO-t (mas. %)	MnO (mas. %)	MgO (mas. %)	CaO (mas. %)	Na_2O (mas. %)	Cr_2O_3 (mas. %)	NiO (mas. %)	V_2O_3 (mas. %)	Total (mas. %)	Mg# (mol %)	Number of analyses
Ol	As-3-OL-1	39.21			17.66	0.33	42.71	0.34			0.20		100.5	81.2	1
Ol	As-3-OL-2	38.71			17.20	0.35	42.26	0.31			0.20		99.0	81.4	1
CPx	As-3-CPx-1b	49.28	1.41	5.39	5.81	0.15	14.51	21.82	0.48	0.5			99.2	81.7	2
(Cr+Ti)-Sp	As-3-Sp-1	0.22	12.86	9.62	55.00	0.37	9.02			8.8	0.24	0.54	96.7		1
(Cr+Ti)-Sp	As-3-Sp-2	0.18	9.01	9.25	56.13	0.37	7.74			12.1		0.35	95.1		1

Figure S4

Comparison of the compositions of olivine phenocrysts in the basanite of Possession Island, obtained using two analytical methods: electron microprobe analysis (Geological Faculty of Lomonosov Moscow State University) **(EMPA, MSU)** and scanning electron microscope TESCAN (GEOKHI RAS) **(TESCAN, GEOKHI RAS)**. Tables with olivine compositions from this work are given in ***Electronic Supplementary-1, Table S2***).

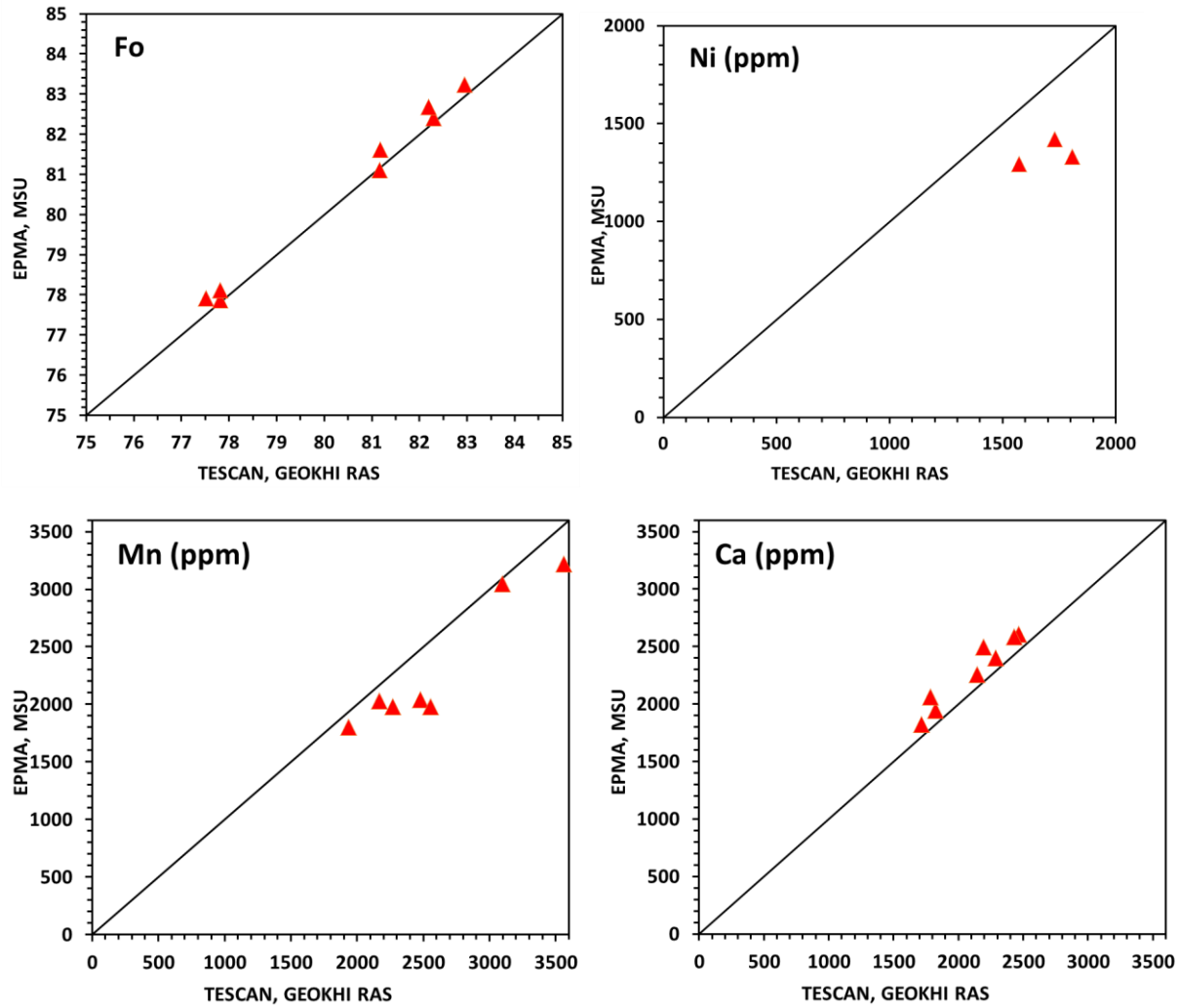

Fig. S4-a. Comparison of the compositions of the same olivine phenocrysts of Possesion basanite P-1-6 analyzed by two methods: **EMPA, MSU and TESCAN, GEOKHI RAS.**

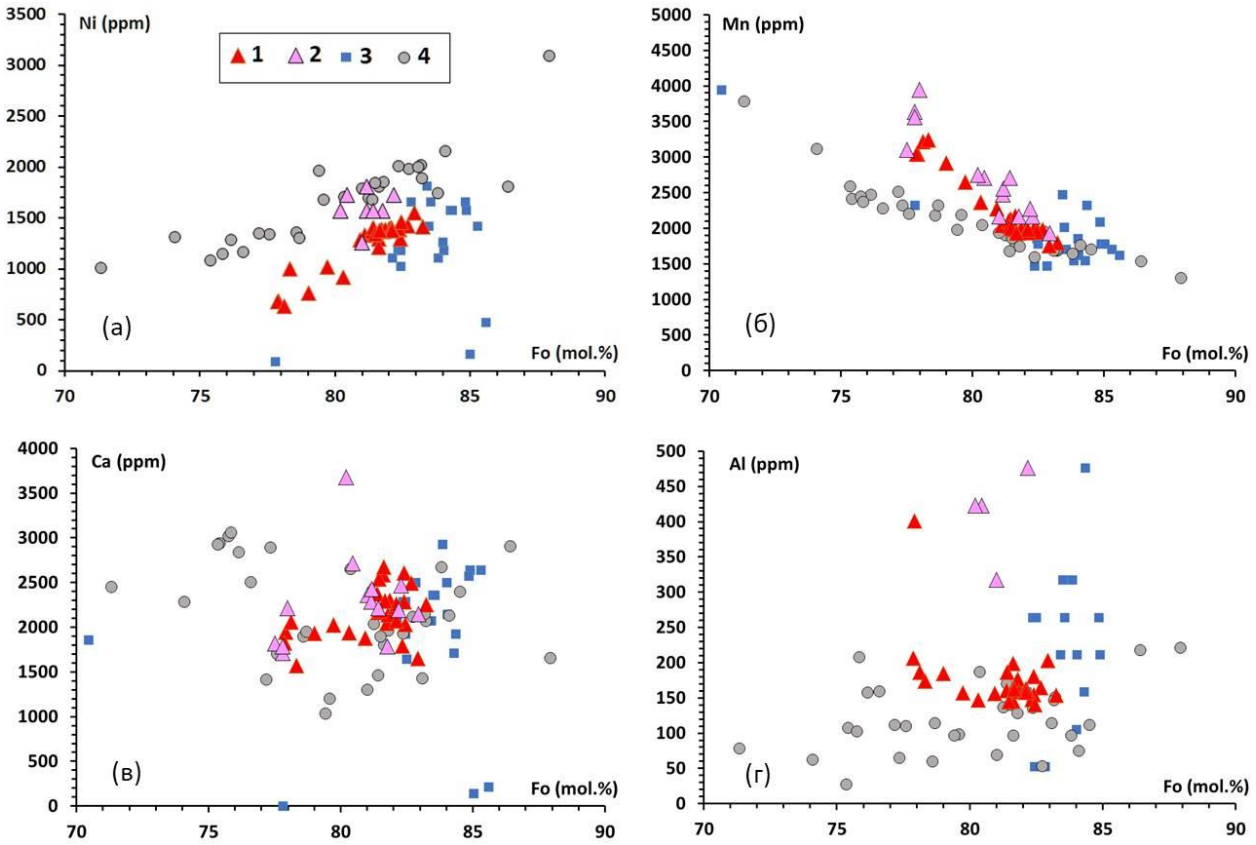

Fig. S4-b. Comparison of compositions of all olivine phenocrysts from Possession Island analysed by two methods in this work with literature data. 1 – Electron Microprobe (EMPA, MSU, our data); 2 – Scanning Electron Microscope (TESCAN, GEOKHI RAS, our data); 3 – olivines from Possession Island (Breton et al., 2013); 4 – olivines from East Island (Crozet Rise) (Meyzen et al., 2016).

Figure S5

Zoned clinopyroxene phenocrysts (two grains) in basanite (sample P-1-6) from Possession Island, with more Fe-rich cores and more Mg-rich rims.

(a) – (b) – Micrographs of the phenocryst, in which Profile-1 was analyzed. The white dashed lines indicate the location of craters after LA-ICP-MS analysis;

(c) – (d) – Micrographs of the phenocryst, in which Profile-2 was analyzed;

(e – m) Variations in the composition of zoned clinopyroxene phenocrysts along the "core – rim" profiles. The data were obtained using Electron Microprobe Analysis (Geological Department of Lomonosov Moscow State University (***Electronic Supplementary-1, Table S4***).

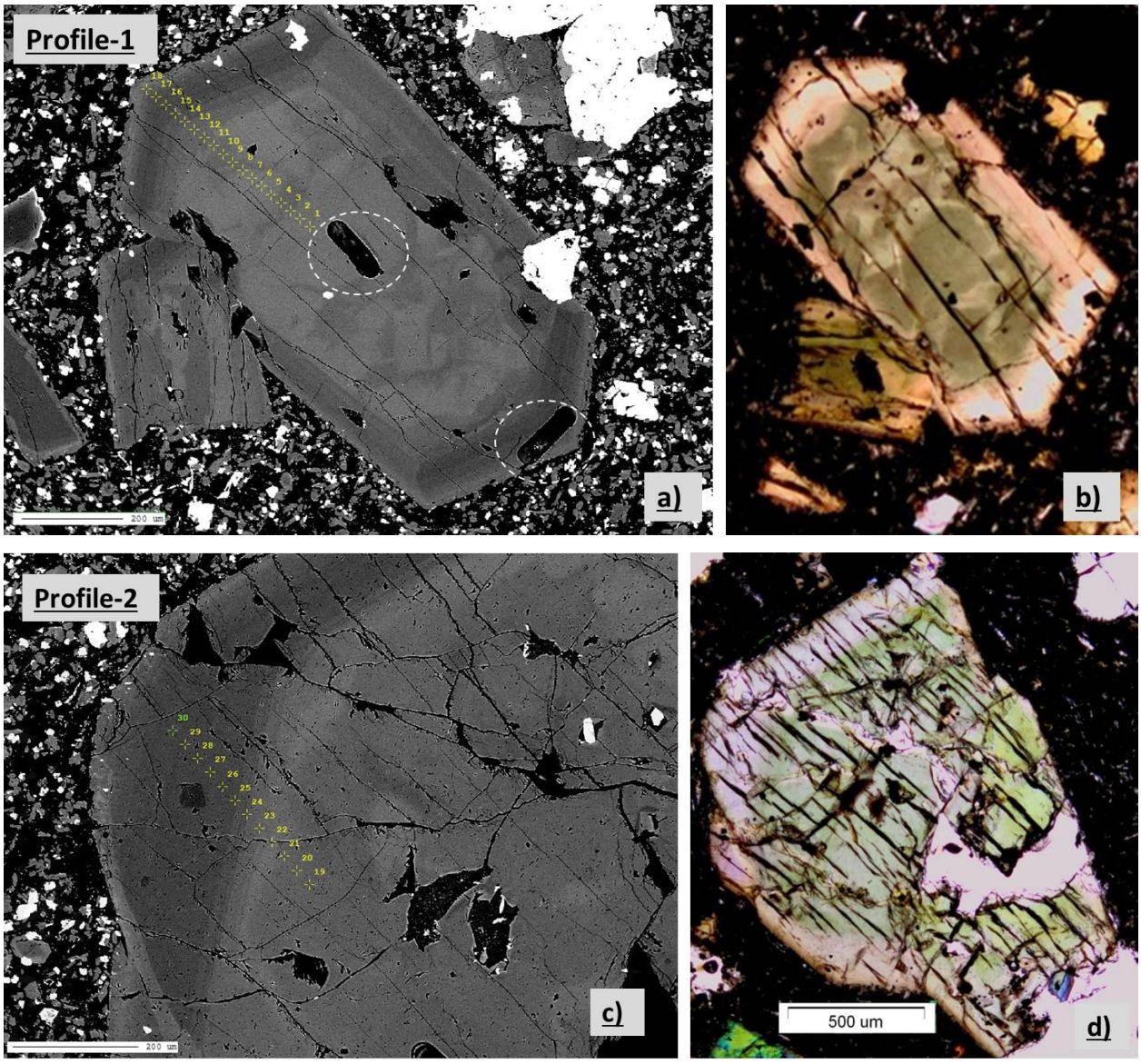

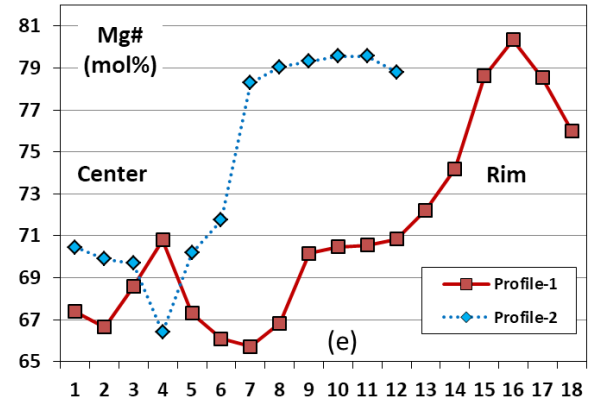
Mg#
(mol%)
Center
Rim
Profile-1
Profile-2
(e)

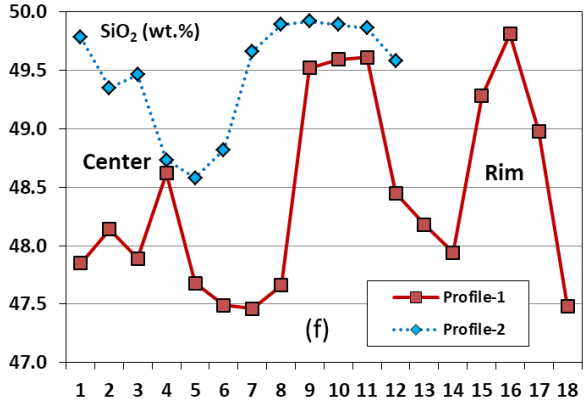
SiO2 (wt.%)
Center
Rim
Profile-1
Profile-2
(f)

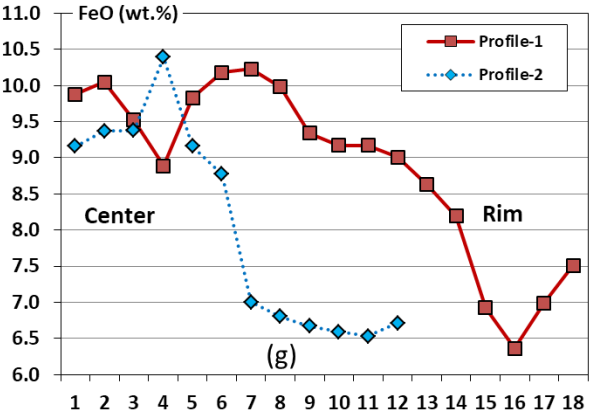
FeO (wt.%)
Center
Rim
Profile-1
Profile-2
(g)

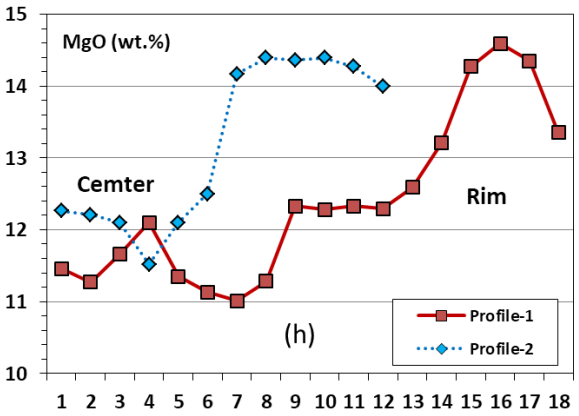
MgO (wt.%)
Cemter
Rim
Profile-1
Profile-2
(h)

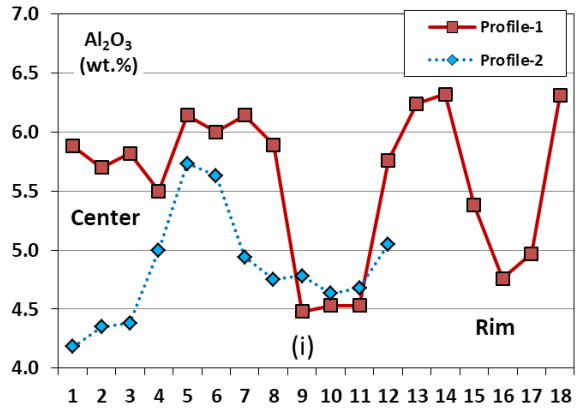
Al2O3
(wt.%)
Center
Rim
Profile-1
Profile-2
(i)

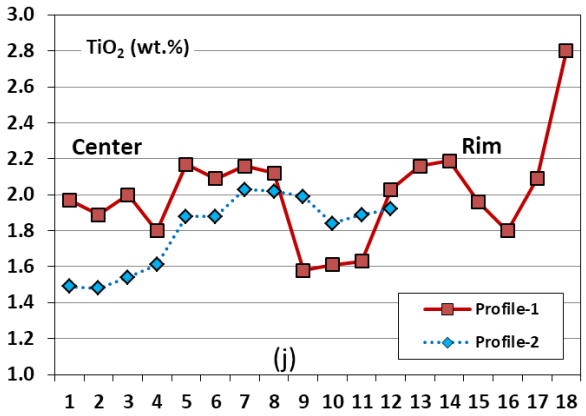
TiO2 (wt.%)
Center
Rim
Profile-1
Profile-2
(j)

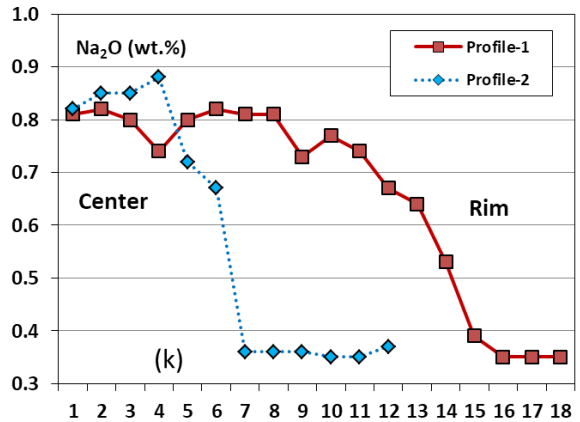
Na2O (wt.%)
Center
Rim
Profile-1
Profile-2
(k)

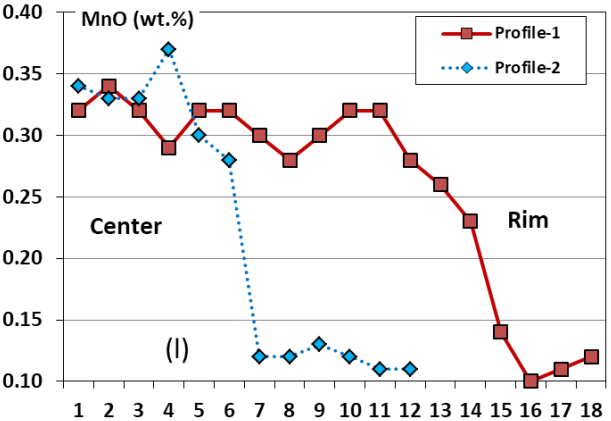
MnO (wt.%)
Center
Rim
Profile-1
Profile-2
(l)

Figure S6

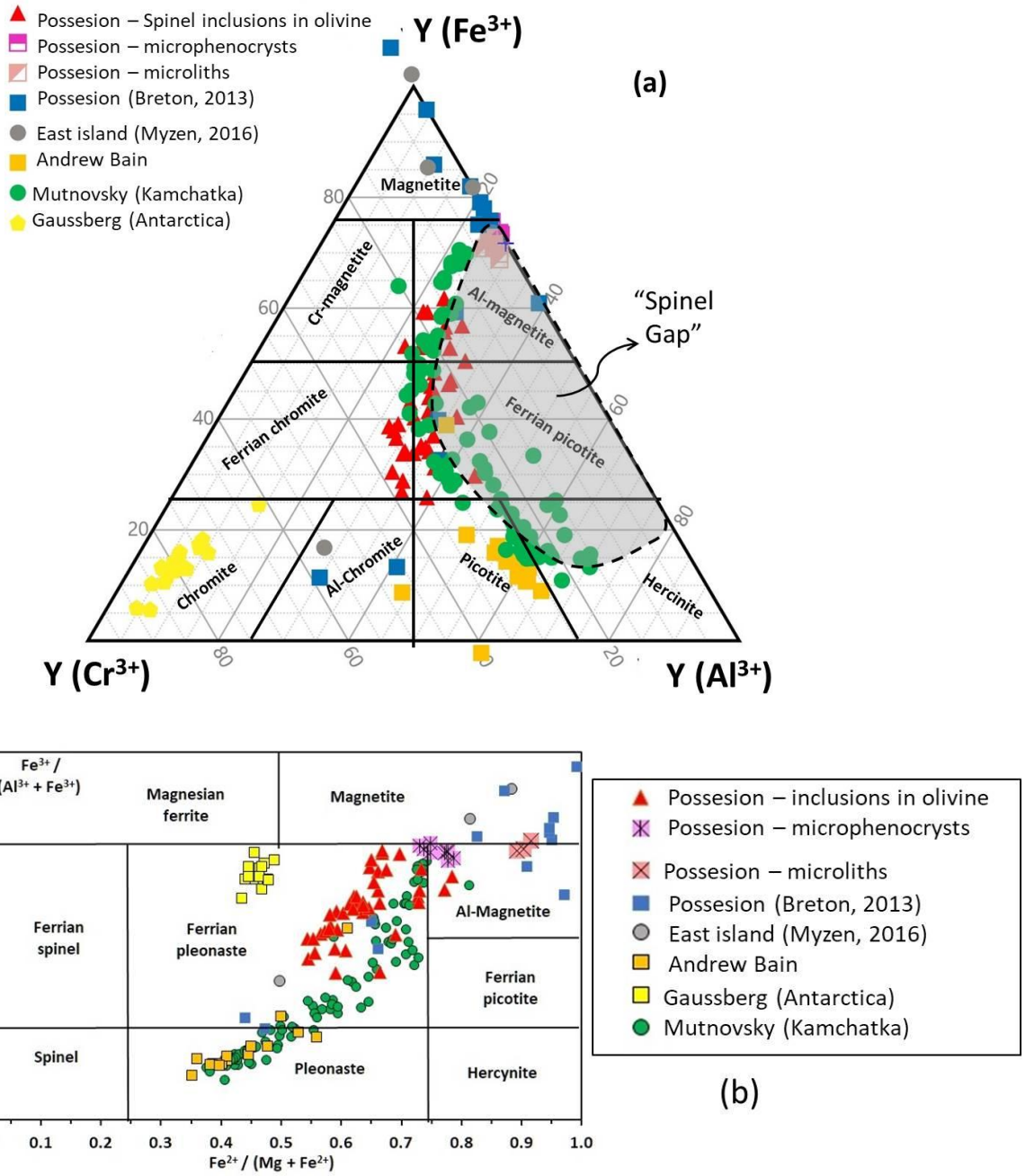

Fig. S6. Compositions of spinel group minerals in basanites from Possession Island compared with data from other localities. Tables with olivine compositions from this work are given in ***Electronic Supplementary-1, Table S5***).The mineral compositions are plotted on classification diagrams for spinel group minerals:

(a) ternary diagram «Cr^{3+}–Fe^{3+}–Al^{3+}» ($Y(Cr^{3+})$ = Cr/(Cr+Fe^{3+}+Al); $Y(Fe^{3+})$ = Fe^{3+}/(Cr+Fe^{3+}+Al); $Y(Al^{3+})$ = Al/(Cr+Fe^{3+}+Al);

(b) binary diagram Fe^{3+}/(Al + Fe^{3+}) vs. Fe^{2+}/(Mg^{2+}+Fe^{2+}).

The fields of mineral types in the diagrams are plotted according to Deer et al. (1992), the "spinel gap" field - according to Barnes and Roeder (2001). The examples of the diagrams are taken from Gargiulo et al. (2013). Literature data are given for: Possession Island - Breton et al. (2013); East Island (Crozet) - Meyzen et al. (2016); Andrew-Bain (SWIR) – Suschevskaya et al. (2024); Gaussberg volcano (Antarctica) – Migdisova et al. (2023); Mutnovsky volcano (Kamchatka) – Shishkina et al. (2018).

Cited literature

Barnes, S.J., Roeder, P.L. (2001) The range of spinel compositions in terrestrial mafic and ultramafic rocks. Journal of Petrology, 12, p. 2279-2302.

Breton, T., Pichat, S., Moine, B., Moreira, M., Rose-Koga, E. F., Auclair, D., Bosq, C. & Wavrant, L.-M. (2013) Geochemical heterogeneities within the Crozet hotspot. Earth Planet. Sci. Lett. 376, p. 126–136.

Deer, W.A., Howie, R.A., Zussman, J. (1992) An introduction to the rock-forming minerals. Harlow, England, ed. Longman Scientific & Technical, 695pp.

Gargiulo M.F., Bjerg E.A. Mogessie A. (2013) Spinel group minerals in metamorphosed ultramafic rocks from Río de Las Tunas belt, Central Andes, Argentina. Geologica Acta, Vol. 11, N2, p.133-148, DOI: 10.1344/105.000001836

Meyzen C. M., Marzoli A., Bellien G and Levresse G. (2016) Magmatic Activity on a Motionless Plate: the Case of East Island, Crozet Archipelago (Indian Ocean) J. Petrol. 57, (7), p. 1409–1436.

Shishkina T.A., Portnyagin M.V., Botcharnikov R.E., Almeev R.R., Simonyan A.V., Garbe-Schönberg D., Schuth S., Oeser M., Holtz F. (2018) Experimental calibration and implications of olivine-melt vanadium oxybarometry for hydrous basaltic arc magmas. Am. Mineral. 103, p. 369-383.

Migdisova, N.A., Sushchevskaya, N.M., Portnyagin, M.V., Shishkina T.A., Kuzmin D.V., Batanova V.G. (2023) Composition of Phenocrysts in Lamproites of Gaussberg Volcano, East Antarctica. Geochem. Int. 61, p. 911–936. https://doi.org/10.1134/S0016702923090082

Sushchevskya N.M., Scherbakov V.D., Peive A.A., Dubinin E. P., B.V. Belyatsky, Zhilkina A.V. (2024) Formation of ceanic crust within the Andrew Bain fault zone of the Southwest Indian ridge (etrological and geochemical data). Geochem. Int., 62 (1), p. 1–17.